



CHORUS

This is the accepted manuscript made available via CHORUS. The article has been published as:

Correction of Phase Errors in a Spin-Wave Transmission Line by Nonadiabatic Parametric Pumping

Roman Verba, Mario Carpentieri, Yu-Jin Chen, Ilya N. Krivorotov, Giovanni Finocchio, Vasil Tiberkevich, and Andrei Slavin

Phys. Rev. Applied **11**, 054040 — Published 15 May 2019

DOI: [10.1103/PhysRevApplied.11.054040](https://doi.org/10.1103/PhysRevApplied.11.054040)

Correction of phase errors in a spin wave transmission line by nonadiabatic parametric pumping

Roman Verba,^{1,*} Mario Carpentieri,² Yu-Jin Chen,³ Ilya N. Krivorotov,³
Giovanni Finocchio,⁴ Vasil Tiberkevich,⁵ and Andrei Slavin⁵

¹*Institute of Magnetism, Kyiv 03142, Ukraine*

²*Department of Electrical and Information Engineering, Politecnico di Bari, I-70125 Bari, Italy*

³*Department of Physics and Astronomy, University of California, Irvine, California 92697, United States*

⁴*Department of Electronic Engineering, Industrial Chemistry and Engineering, University of Messina, I-98166 Messina, Italy*

⁵*Department of Physics, Oakland University, Rochester, MI 48309, USA*

It is shown that phase errors in a microwave spin wave transmission line can be corrected by subjecting the signal-carrying propagating spin wave to the action of a localized nonadiabatic parametric pumping, having the localization length smaller than the spin wave wavelength. In such a transmission line the phase transmission characteristic has a “step-like” shape containing flat “stabilization plateaus” separated by the intervals of the π -size. Within the “plateau” regions the phase of the output spin wave is practically constant in a rather wide range of phases of the input spin wave. This effect can be used in magnonic logic devices for the correction of phase errors of up to $\pm 0.25\pi$. It is also proved, that this phase stabilization effect is stable against the variations of the spin wave amplitude, and is present in all the amplitude range of the stable spin wave propagation.

I. INTRODUCTION

Spin waves (SWs) propagating in nanoscale ferromagnetic waveguides are considered to be promising for the applications in a new generation of digital and analog signal processing devices [1–5]. Recently, several novel concepts of magnonic logic elements and circuits have been proposed [6–12]. In magnonic logic, a digital signal can be coded via SW amplitude [6, 13–15] or SW phase [2, 16]. Obviously, in the case of phase-coded magnonic logic devices the spin wave phase should be well-defined, and should not fluctuate substantially in the course of the spin wave propagation. This property of the SW phase stability is also crucial for amplitude-coded magnonic logic devices. Indeed, these devices often use SW interference for the information processing, and the phase relations between several processed SWs should be well-defined for correct device operation [13, 15, 17, 18].

For example, result of the interference of two SWs having phases φ_1 , φ_2 and similar amplitudes is proportional to $\cos[(\varphi_1 - \varphi_2)/2]$. Deviation of the phase difference by 0.55π could be enough for incorrect interpretation of the interference result – instead of 1 in the ideal case $\varphi_1 - \varphi_2 = 0$ (or 0 if $\varphi_1 - \varphi_2 = \pi$) the resulting signal becomes lesser than $2/3$ (greater than $1/3$), which is commonly interpreted as indeterminate in the amplitude-coded logic [15]. Deviation of the phase difference by 0.8π leads to a completely wrong result – logic “0” instead of “1” and vice versa.

There are several reasons for the SW phase deviation in a magnonic circle. First is the deviation of the SW waveguide length due to lithographic misprints. It can occur, for example, due to a misposition of waveguide bends and a spread of bends shape in a circuit. Small

length deviations, not exceeding 1 nm at each bend, can accumulate over a magnonic circle and, for exemplary SW of the 100 nm wavelength, could reach critical value (corresponding to 0.55π phase shift) after passing several tens of such bends. Similarly, misprint of the waveguide width leads to a change of SW dispersion and, thus, SW wavenumber at a fixed frequency, which is another source of random phase accumulation. Finally, stability of the SW phase can be violated by thermal fluctuations, and the phase deviations leading, eventually, to a signal processing error, can accumulate in the course of the SW propagation in a magnonic circuit. Therefore, the timely correction of the phase errors is very important for the stable and error-free operation of magnonic logic circuits.

In this work, we demonstrate that the problem of the phase errors correction can be solved by the application of a localized parametric pumping, i.e. by using the interaction of a propagating SW with a localized microwave magnetic field (external or internal) of approximately double SW frequency. Parametric pumping is a well-known method for excitation and amplification of SWs [19–22]. It is also known, that parametric interaction becomes phase-sensitive in the case of a so-called “nonadiabatic” localized pumping, having the localization length (or other characteristic length of the spatial variation) that is smaller than the SW wavelength [23–25]. In our current work we calculate the phase transmission characteristics for an SW transmission line containing a region where a nonadiabatic parametric pumping is acting, and show that phase transmission characteristics of such a line demonstrate “stabilization plateaus”, within which the phase of the output SW signal is practically constant in a rather wide range of phases of the input SW signal. Thus, the phase fluctuation of the SW signal acquired in the course of its propagation can be corrected. It is important, that these phase-stabilization plateaus are separated by the intervals of the size almost exactly equal

* corresponding author, e-mail: verrv@ukr.net

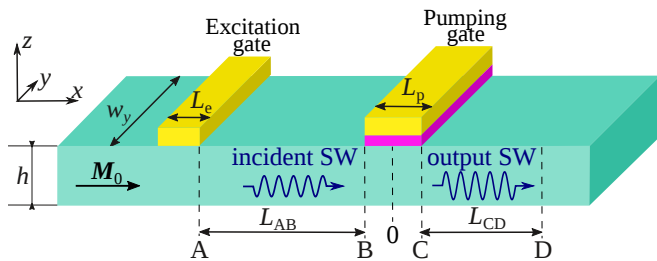


FIG. 1. A sketch of the considered magnonic transmission line showing regions of the SW excitation and the localization of the parametric pumping. The reference points A-D used in the in the micromagnetic simulations are also shown.

to π , thus being perfectly suitable for the phase-coded magnonic logic or/and signal processing.

II. THEORY

A sketch of the considered SW transmission line is shown in Fig. 1. It is a ferromagnetic nanowire of the width w_y and thickness h . The SWs of the frequency ω_k , propagating in the $+x$ direction, are excited by the excitation gate, or, in an integrated magnonic circuit, come from a preceding SW signal processing device. The parametric pumping gate of the length L_p is placed on the propagation path of the SWs. The parametric pumping can be created by a microwave magnetic field with polarization parallel to the direction of static magnetization of the nanowire [20, 21], by the microwave electric field via various magnetoelectric effects [22], or by other means. The phase-stabilization effects discussed below do not depend on the nature of the pumping, and are also independent of the direction of static magnetization of the nanowire.

To be specific with the coefficients used in our calculations, we considered the case of a parametric pumping produced by a microwave voltage via the voltage-controlled magnetic anisotropy effect (VCMA) [26, 27], which is the most efficient and convenient for applications at nanoscale. In this case the pumping gate consists of a strip of a normal metal separated by a dielectric layer from the conductive ferromagnetic material of the nanowire. The application of the microwave voltage of the frequency ω_p to the gate results in oscillations of the perpendicular magnetic anisotropy at the ferromagnetic - dielectric interface with the same frequency [28, 29]. It was shown that these oscillations of anisotropy can couple parametrically to the SWs propagating in the nanowire, both in the case of the in-plane and out-of-plane static magnetization direction of the nanowire [22, 29, 30]. In the former case the coupling is stronger, and demonstrates no limits with respect to the SW wave number [30], so below we consider only this case of the in-plane static magnetization, as shown in Fig. 1.

In the parametric process of the first order the pump-

ing is coupled to a pair of SWs having wave vectors k and k' . The efficiency of the parametric interaction is proportional to the $(k + k')$ -th Fourier harmonic $b_{p,k+k'}$ of the spatial distribution of the effective pumping field $b_p(x)$. Therefore, in the case of a weakly localized quasiniform pumping, when $kL_p \gg 1$, only the SWs with opposite wave vectors, $k' = -k$, interact efficiently with pumping, which is a consequence of the momentum conservation law (case of “adiabatic pumping”).

In contrast, when the pumping localization length L becomes smaller than the SW wavelength (or if the pumping is spatially nonuniform with the characteristic length comparable to the SW wavelength) not only the contra-propagating SWs ($k' = -k$), but also other SWs ($k' \neq k$), in particular, co-propagating SWs, can interact with the localized pumping field. This is the case of “nonadiabatic parametric pumping”, described in Ref. 23.

It should be noted, that the parametric interaction has the maximum efficiency when the resonance condition $\omega_p = \omega_k + \omega_{k'}$ is satisfied. This condition severely limits the number of SWs that can efficiently interact with pumping. In the simple, and the most common case, when the pumping frequency is twice larger than the SW frequency, $\omega_p = 2\omega_k$, the only SWs efficiently interacting with the nonadiabatic pumping are the above mentioned contra-propagating SWs having the same modulus of the SWs wave vectors k and $-k$; however, nonadiabatic term results in additional coupling of these SWs with themselves (that is the limiting case of the coupling of co-propagating SWs, when approaching exact parametric resonance).

The SW dynamics under a localized parametric pumping is convenient to study using Bloembergen’s equations system. For the case of a nonadiabatic pumping it was generalized in Ref. 23, and, neglecting the higher order nonlinear SW interactions, it can be written as:

$$\begin{aligned} \left(\frac{\partial}{\partial t} + v \frac{\partial}{\partial x} + \Gamma \right) a_1 &= V b_0 e^{-i\psi} a_2^* + V b_{2k} e^{-i\psi} a_1^*, \\ \left(\frac{\partial}{\partial t} - v \frac{\partial}{\partial x} + \Gamma \right) a_2^* &= V b_0 e^{i\psi} a_1 + V b_{2k} e^{i\psi} a_2. \end{aligned} \quad (1)$$

This system describes the evolution of the envelope amplitudes $a_1(x, t)$ and $a_2(x, t)$ of the two SW wave packets, having the carrier wave vectors k and $-k$, respectively. In our problem, a_1 describes the envelope amplitude of the incident SW, which propagates toward the pumping region, and a_2 is the envelope amplitude of the idler SW, which is counter-propagating to a_1 , and appears in the pumping region as a result of the parametric interaction. The relation of envelope amplitudes to the real magnetization amplitudes is given by the equation $\mathbf{m}_{1,2}(x, t) = (\mathbf{m}_k a_{1,2}(x, t) \exp[\pm i k x - i \omega_k t] + \text{c.c.})$, where \mathbf{m}_k describes the vector structure (ellipticity) of a particular SWs. In Eq. (1) v and Γ are the group velocity and the damping rate of the SWs, V is the efficiency of the parametric coupling, ψ is the phase of the pumping,

and $b_k = (1/L_p) \int_{-L_p/2}^{L_p/2} b_p(x) e^{ikx} dx$ is Fourier-harmonic of the effective field of pumping with the spatial profile $b_p(x)$. The fact that pumping is nonadiabatic is reflected by the last term in equations, which describes the parametric coupling of the co-propagating SWs ($k' = k$). In the case of quasi-uniform adiabatic pumping this term is, naturally, absent, since $b_{2k} \rightarrow 0$. The value $\alpha = |b_{2k}/b_0|$ describes the strength of the nonadiabatic term relative to the adiabatic one, and is called “the degree of nonadiabaticity of the pumping”.

In our particular case of the in-plane static magnetization and VCMA-induced pumping, the efficiency of the the parametric coupling is given by $V = \gamma|m_{k,z}/4m_{k,y}|$, the pumping field is $b_p = 2\beta E/hM_s$ with β being the magnetoelectric coefficient, E is the amplitude of the microwave electric field applied to the pumping gate [30], while the pumping Fourier-harmonics b_k are given by the expression $b_k = b_p \text{sinc}[kL_p/2] \equiv b_p \sin[kL_p/2]/(kL_p/2)$.

The pumping phase ψ is defined in such a way that the applied microwave electric field is $E(t) = E \sin[\omega_p t + \psi]$, with $\omega_p = 2\omega_k$ (exact parametric resonance). The real dynamic magnetization, corresponding to the steady propagating SW of the envelope amplitude $a_1 = |a_1|e^{-i\varphi}$, is $m_z(x, t) = 2m_{z,k} \sin[\omega_k t + \varphi - kx]$, where φ is the SW phase. Note, that the point $x = 0$ is assumed to be at the center of the pumping gate, as shown in Fig. 1, and its position, obviously, affects the definitions of the phases φ and ψ . For other cases of the parametric pumping source and other directions of the static magnetization, the only differences in Eq. (1) come from the different value of the parametric coupling efficiency V , [19, 21, 22], and relations of the phases ψ and φ to the real time profiles of the dynamic magnetization and applied pumping signal (microwave magnetic or electric field).

For further analysis it is convenient to introduce new real variables $A_{1\pm}$, $A_{2\pm}$, as $a_1 = e^{-i\psi/2}(A_{1+} + iA_{1-})$ and $a_2 = e^{-i\psi/2}(A_{2+} - iA_{2-})$, which is possible if the pumping is harmonic, i.e. if the pumping phase is time-independent, $\psi \neq \psi(t)$. This operation, in fact, is a decomposition of a harmonic wave with an arbitrary phase into two partial waves, sine and cosine, respectively. Then, Eq. (1) is transformed to [23]:

$$\begin{aligned} \left(\frac{\partial}{\partial t} + v \frac{\partial}{\partial x} + \Gamma \mp Vb_{2k} \right) A_{1\pm} &= Vb_0 A_{2\pm}, \\ \left(\frac{\partial}{\partial t} - v \frac{\partial}{\partial x} + \Gamma \mp Vb_{2k} \right) A_{2\pm} &= Vb_0 A_{1\pm}. \end{aligned} \quad (2)$$

As one can see, the pairs of partial waves (A_{1+} , A_{2+}) and (A_{1-} , A_{2-}) evolve independently, and are connected only by the boundary conditions. The action of the nonadiabatic term Vb_{2k} results in the different effective damping for partial waves: effective damping for the “in-phase” partial waves (A_{1+} , A_{2+}) is decreased, while the “out-of-phase” SWs (A_{1-} , A_{2-}) acquire an additional damping term. Thus, the partial waves evolve differently under the action of pumping, since the pumping pumps energy more effectively into the “in-phase” partial waves.

To find a steady-state solution of the transmission problem, we consider a stationary regime, setting $\partial A_i / \partial t = 0$. Equations (2) should be accompanied by a boundary condition: $a_1(-L_p/2) = A_0 e^{-i\varphi_0}$, which describes the incoming SW with amplitude A_0 and arbitrary phase φ_0 , and $a_2(L_p/2) = 0$, meaning that no idler wave is incident to the pumping region. Then, the envelope amplitude of the output SW $a_{\text{out}} = a_1(L_p/2)$ can be found as:

$$a_{\text{out}} = A_0 e^{-i\psi/2} \left(\cos \left[\varphi_0 - \frac{\psi}{2} \right] K_+ - i \sin \left[\varphi_0 - \frac{\psi}{2} \right] K_- \right), \quad (3)$$

where

$$K_{\pm} = \left(\cos[\kappa_{\pm} L_p] + \frac{\tilde{\Gamma}_{\pm}}{v\kappa_{\pm}} \sin[\kappa_{\pm} L_p] \right)^{-1} \quad (4)$$

are the amplification rates for partial waves, $\tilde{\Gamma}_{\pm} = \Gamma \mp Vb_{2k}$, and $\kappa_{\pm}^2 = (Vb_0)^2 - \tilde{\Gamma}_{\pm}^2$.

As usual[21], the parametric pumping results in a partial amplification of the incident SW, until pumping amplitude reaches a certain threshold, at which a spontaneous generation of SWs takes place (the threshold of generation is determined from the condition $K_+ \rightarrow \infty$). Due to the nonadiabatic term, the amplification rates of the partial waves are different, resulting in the dependence of the output SW amplitude on its phase [23, 24]. Simultaneously, it means that the ratio between the amplitudes of the partial waves A_{1+} and A_{1-} changes within the pumping region, and is different at the end of the pumping gate compared to the gate entrance. Thus, the phase of the incident SW a_1 changes during the propagation through the pumping gate. Since the “in-phase” partial wave A_{1+} grows faster (or decays slower) than the “out-of-phase” partial wave, the phase of the incident wave approaches the phase of the “in-phase” partial wave, which is fixed by the phase of pumping to the accuracy of an integer multiple of π : $\varphi(x) \rightarrow \psi/2 + \pi n$, $n \in \mathbb{Z}$.

The phase transmission characteristics are obtained from Eq. (3), simply as $\varphi_{\text{out}} = -\text{Arg}[a_{\text{out}}]$. In the case of an adiabatic pumping, when $b_{2k} = 0$, the phase transmission characteristic is a simple straight line, $\varphi_{\text{out}} = \varphi_0$ (Fig. 2(a)). Recall, that the SW phase φ was introduced as a phase of the SW envelope, so the propagation phase shift kL_p is not taken into account in Fig. 2. This leads to a simple vertical shift of all the curves.

In contrast, as soon as the pumping becomes nonadiabatic, the SW phase transmission characteristics become nonlinear. They demonstrate pronounced plateaus near the values $\varphi = 0, \pi$, which are the phases of the “in-phase” partial wave (since it was assumed that the pumping phase $\psi = 0$). Within these plateaus, the output SW phase is almost constant in a wide range of the input SW phases, i.e. the nonadiabatic parametric pumping

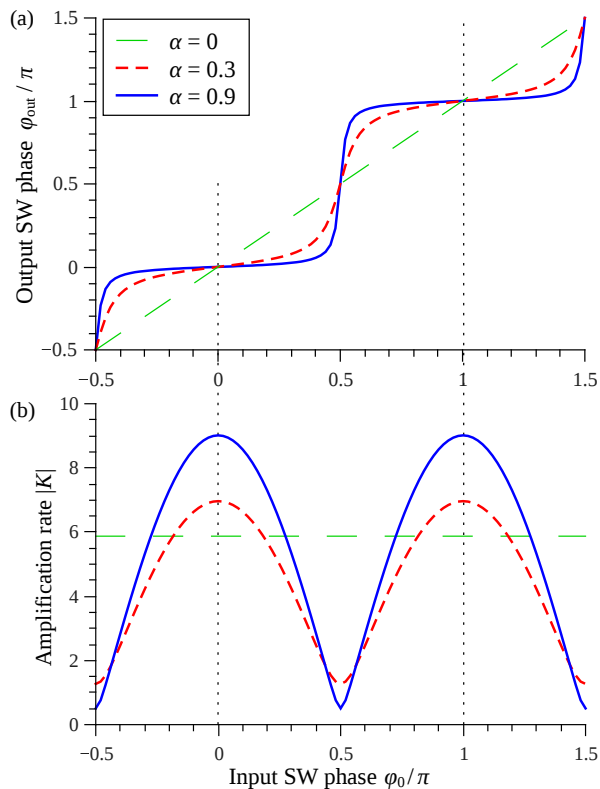


FIG. 2. (a) SW phase transmission characteristics $\varphi_{out} = f(\varphi_0)$ and (b) amplification rates $|K| = f(\varphi_0)$ of a parametric pumping gate for different degrees of the pumping nonadiabaticity $\alpha = |b_{2k}/b_0|$. Pumping length $L_p = 0.1v/\Gamma$, pumping strength is the 90% of the SW generation threshold, pumping phase $\psi = 0$.

demonstrates the effect of a SW phase stabilization. Importantly, the SW phase stabilization plateaus are separated by the phase intervals of the π -size, which perfectly matches the needs of the phase-coded magnonic logic, as under this approach the logic state “0” and the logic state “1” are coded by the SWs with the phase difference of π .

Stabilization plateaus become wider and more flat with the increase in the degree $\alpha = |b_{2k}/b_0|$ of the pumping “nonadiabaticity” (Fig. 2(a)). A similar enhancement of the phase stabilization properties is observed with the increase of the pumping strength, when this strength approaches the threshold of the parametric SW generation. In a limiting case, when $K_+ \gg K_-$ (which means that the pumping amplitude is close to the threshold, or that the length of the pumping region is sufficiently large), the phase transmission characteristic becomes almost a step-like function.

It should be noted, that the pumping nonadiabaticity also results in the dependence of the output SW amplitude on the input SW phase, as shown in Fig. 2(b). When the phase stabilization becomes better, the variations of the SW amplitude also increase. Large variations of the SW amplitude, naturally, are not acceptable

in the SW processing devices, which limits the practically achievable ranges of the possible phase error corrections. Usually, about 10-15 % of the SW amplitude variation can be considered acceptable, which defines practical limits of the possible phase error correction interval as about $\pm 0.25\pi$. Additional improvements can be achieved by placing after the phase stabilizer a phase-insensitive amplitude-stabilization device, which could use a nonlinear regime of the SW interaction with adiabatic pumping [31] or other nonlinear phenomena.

At the same time, a certain degree of the SW amplitude variation can even be useful. When the SW phase is close to $\varphi_0 = \pi/2$, it means that the phase error is large, and the interpretation of the SW phase as the closest value of 0 or π may be incorrect. In a case of so large values of the phase errors it is often recommended to start the signal processing over. The above proposed phase-stabilization device indicates such large phase errors by a significant reduction of the amplitude of the output SW. In summary, using the proposed phase-stabilization device small and moderate phase errors can be corrected, while the presence of large phase errors can clearly determined and indicated.

Finally, we note that Fig. 2 illustrates the case when the phase stabilization is accompanied by the amplification of processed SWs. Often, this amplification is desirable in magnonic circuits to compensate propagation and processing losses, but sometimes a regime of no amplification ($K(0, \pi) \approx 1$) for in-phase waves needs to be realized. Fortunately, it is easy to vary the SW amplification rate by choice of the pumping amplitude and length. For example the case of no amplification requires either a sufficiently long parametric pumping gate or the enhanced magnetic damping within the parametric gate, so that the “out-of-phase” partial SWs decay significantly. The pumping nonadiabaticity in the case of a relatively long pumping gates can be realized by creating a spatially nonuniform pumping (e.g. pumping gate consisting of several fingers having different polarity and/or strength of applied voltage). If the averaged pumping signal is nonzero (e.g., if fingers of opposite polarity are of unequal length), SW dynamics is described by the same Eq. (1), in which nonadiabatic term b_{2k} becomes large if $2k \approx 2\pi/P$, where P is the period of the fingers array. However, even in the case of zero averaged pumping one should expect the phase stabilization effect. In this case only nonadiabatic term is left, and one arrives to the limiting case the parametric interaction of co-propagating waves, when idler wave is equivalent to the signal wave. In the case of co-propagating waves parametric pumping also can amplify waves (but cannot excite them) [32, 33], and nonadiabatic term still be phase-sensitive; thus, one should expect qualitatively the same effect.

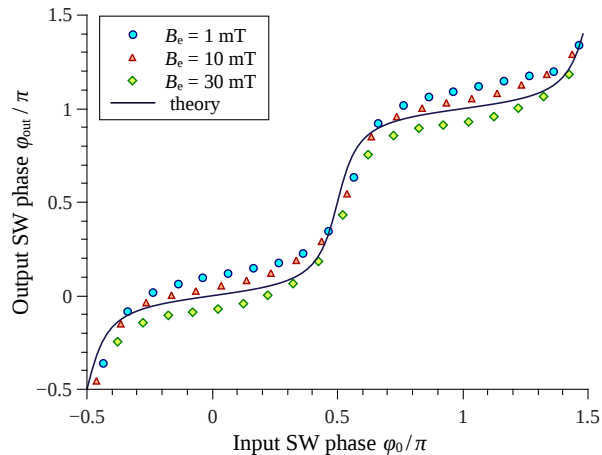


FIG. 3. Phase transmission characteristics of a VCMA parametric pumping gate for different incident SW amplitudes created by the different excitation fields B_e (symbols – micromagnetic simulations, solid line – theoretical curve for linear SWs.)

III. MICROMAGNETIC SIMULATIONS

To confirm our theoretical predictions about the SW phase stabilization we performed a series of micromagnetic simulations using the GPMagnet solver [34, 35]. In our simulations the SWs were excited linearly by a microwave magnetic field applied at the excitation gate of the length $L_e = 50$ nm. The excitation frequency was 6.49 GHz which corresponds to the SW wavelength of 210 nm. The microwave parametric pumping in the form of modulation of the perpendicular anisotropy $\Delta K_{\perp} = b_p M_s \sin[\omega_p t]$ at the frequency $\omega_p/(2\pi) = 12.98$ GHz was applied at the pumping gate of the length $L_p = 50$ nm, separated from the excitation gate by the distance $L_{AB} = 250$ nm. Corresponding degree of the pumping nonadiabaticity in this case is $\alpha = 0.67$. To avoid the mistakes in the output SW phase determination due to the presence of the idler SW, the phase of the output SW was calculated at the point D. The SW phase at the end of the gate was retrieved by subtraction of the propagation phase accumulation kL_{CD} , where $L_{CD} = 250$ nm. The following material parameters of the Fe/MgO structure (common for VCMA experiments [36]) were used: saturation magnetization $\mu_0 M_s = 2.1$ T, exchange length $\lambda_{ex} = 3.4$ nm, surface perpendicular anisotropy energy $K_s = 1.36$ mJ/m², effective Gilbert damping (including non-uniform broadening for a given SW frequency) $\alpha_G = 0.02$. The nanowire thickness was set to $h = 1$ nm, width $w = 20$ nm, and the bias magnetic field was absent.

Simulations performed with no incident SW and finite temperature of 1 K give the threshold of parametric excitation equal to $b_{p,th} = 130$ mT. It is somewhat smaller, than the threshold of 169 mT, calculated using the analytical equation Eq. (4) (from the condition $K_+ \rightarrow \infty$). We believe, that the discrepancy is caused by the dispersion of SW group velocity.

In the simulations of the SW phase transmission characteristics in the presence of an incident SW we set the pumping strength to $b_p = 100$ mT, which is 77% of the SW generation threshold. Thermal fluctuation were switched off to speed up the simulations – since we work sufficiently away from the threshold we do not expect a significant growth of thermal fluctuations under the parametric pumping gate. Simulated phase transmission characteristic for small-amplitude (linear) SWs, which were excited by a 1 mT excitation field, is shown in Fig. 3 (blue dots). It shows definite phase-stabilization plateaus, and matches well the phase characteristic obtained in the analytical calculation (solid line) for the pumping strength equal to 77% of theoretical SW generation threshold. We believe, that the small upshift of the simulated phase characteristic is also related with the dispersion of the SW group velocity.

We have also verified how phase transmission characteristics change with the SW amplitude, when different nonlinear SW interactions become important. For this purpose we performed simulations for larger excitation fields, 10 mT and 30 mT, respectively. For the excitation field of 30 mT the SW amplitude reaches the value $M_y/M_s \approx 0.15$, which is definitely beyond the range where the excited SWs can be considered small-amplitude (or linear) and in which our analytical theory is valid. From Fig. 3 one can see that the phase-stabilization effect is still present in the case of the large-amplitude nonlinear SWs, and the sizes and slope of the phase-stabilization plateaus are almost the same, as in the linear case. The only difference is a down-shift of these plateaus, which is a consequence of the nonlinear SW phase accumulation. Thus, the nonadiabatic parametric pumping can be used for phase error correction of both linear and nonlinear SWs.

IV. SUMMARY

In summary, we have demonstrated that the interaction of a propagating SW with a localized nonadiabatic parametric pumping leads to a shift of the SW phase, additional to a simple propagation phase accumulation kL_p . As a result, the SW phase transmission characteristics become nonlinear, demonstrating a “step-like” shape. They contain pronounced flat “stabilization plateaus”, within which the output SW phase is almost constant in a certain range of phases of the input SW. The phase-stabilization effect becomes more pronounced with the increased level of the pumping nonadiabaticity, and when the pumping strength approaches the threshold of the parametric SW generation (but it should not exceed the threshold). Our findings open a way for the implementation of phase error corrections in magnonic logic circuits. The range of possible phase error correction is limited mainly by the phase dependence of the output SW amplitude, and is about $\pm 0.25\pi$, for both linear and nonlinear SWs.

ACKNOWLEDGMENTS

This work was supported in part by Grants No. EFMA-1641989, No. ECCS-1708982, No. DMR-1610146 from the U.S. NSF, and by the DARPA M3IC grant under Contract No. W911-17-C-0031. R.V. acknowledges support from the Ministry of Education and Sci-

ence of Ukraine (Project No. 0118U004007). I.N.K. acknowledges support by the Army Research Office through Grant No. W911NF-16-1-0472 and by the Defense Threat Reduction Agency through Grant No. HDTRA1-16-1-0025. G.F. and M.C. would like to acknowledge the contribution of the COST Action CA17123 “Ultrafast opto magneto electronics for non-dissipative information technology”.

-
- [1] V. V. Kruglyak, S. O. Demokritov, and D. Grundler, “Magnonics,” *J. Phys. D: Appl. Phys.* **43**, 264001 (2010).
- [2] A. Khitun, M. Bao, and K. L. Wang, “Magnonic logic circuits,” *J. Phys. D: Appl. Phys.* **43**, 264005 (2010).
- [3] S. O. Demokritov and A. N. Slavin, eds., *Magnonics. From Fundamentals to Applications* (Springer, Berlin, 2013).
- [4] D. E. Nikonov and I. A. Young, “Overview of Beyond-CMOS Devices and a Uniform Methodology for Their Benchmarking,” *Proc. IEEE* **101**, 2498 (2013).
- [5] M. Krawczyk and D. Grundler, “Review and prospects of magnonic crystals and devices with reprogrammable band structure,” *J. Phys.: Cond. Matter* **26**, 123202 (2014).
- [6] A. V. Chumak, A. A. Serga, and B. Hillebrands, “Magnon transistor for all-magnon data processing,” *Nat. Commun.* **5**, 4700 (2014).
- [7] A. V. Chumak, V. I. Vasyuchka, A. A. Serga, and B. Hillebrands, “Magnon spintronics,” *Nat. Phys.* **11**, 453 (2015).
- [8] S. Dutta, S.-C. Chang, N. Kani, D. E. Nikonov, S. Manipatruni, I. A. Young, and A. Naeemi, “Non-volatile Clocked Spin Wave Interconnect for Beyond-CMOS Nanomagnet Pipelines,” *Sci. Rep.* **5**, 9861 (2015).
- [9] A. Khitun, “Parallel database search and prime factorization with magnonic holographic memory devices,” *J. Appl. Phys.* **118**, 243905 (2015).
- [10] K. Ganzhorn, S. Klingler, T. Wimmer, S. Geprägs, R. Gross, H. Huebl, and S. T. B. Goennenwein, “Magnon-based logic in a multi-terminal YIG/Pt nanostructure,” *Appl. Phys. Lett.* **109**, 022405 (2016).
- [11] A. V. Sadovnikov, S. A. Odintsov, E. N. Beginin, S. E. Sheshukova, Yu. P. Sharaevskii, and S. A. Nikitov, “Toward nonlinear magnonics: Intensity-dependent spin-wave switching in insulating side-coupled magnetic stripes,” *Phys. Rev. B* **96**, 144428 (2017).
- [12] Q. Wang, P. Pirro, R. Verba, A. Slavin, B. Hillebrands, and A. V. Chumak, “Reconfigurable nanoscale spin-wave directional coupler,” *Sci. Adv.* **4**, e1701517 (2018).
- [13] T. Schneider, A. A. Serga, B. Leven, B. Hillebrands, R. L. Stamps, and M. P. Kostylev, “Realization of spin-wave logic gates,” *Appl. Phys. Lett.* **92**, 022505 (2008).
- [14] B. Lenk, H. Ulrichs, F. Garbs, and M. Münzenberg, “The building blocks of magnonics,” *Phys. Rep.* **507**, 107 (2011).
- [15] Q. Wang, R. Verba, T. Brächer, P. Pirro, and A. V. Chumak, “Integrated magnonic half-adder,” *ArXiv:1902.02855 [physics.app-ph]*.
- [16] S. Klingler, P. Pirro, T. Brächer, B. Leven, B. Hillebrands, and A. V. Chumak, “Spin-wave logic devices based on isotropic forward volume magnetostatic waves,” *Appl. Phys. Lett.* **106**, 212406 (2015).
- [17] M. Balynsky, A. Kozhevnikov, Y. Khivintsev, T. Bhowmick, D. Gutierrez, H. Chiang, G. Dudko, Y. Filimonov, G. Liu, C. Jiang, A. A. Balandin, R. Lake, and A. Khitun, “Magnonic interferometric switch for multi-valued logic circuits,” *J. Appl. Phys.* **121**, 024504 (2017).
- [18] B. Rana and Y. Otani, “Voltage-Controlled Reconfigurable Spin-Wave Nanochannels and Logic Devices,” *Phys. Rev. Applied* **9**, 014033 (2018).
- [19] V. S. L’vov, *Wave Turbulence under Parametric Excitation* (Springer-Verlag, New York, 1994).
- [20] A. G. Gurevich and G. A. Melkov, *Magnetization Oscillations and Waves* (CRC Press, New York, 1996) p. 464.
- [21] T. Brächer, P. Pirro, and B. Hillebrands, “Parallel pumping for magnon spintronics: Amplification and manipulation of magnon spin currents on the micron-scale,” *Phys. Rep.* **699**, 1–34 (2017).
- [22] R. Verba, M. Carpentieri, G. Finocchio, V. Tiberkevich, and A. Slavin, “Chapter13 - Parametric Excitation and Amplification of Spin Waves in Ultrathin Ferromagnetic Nanowires by Microwave Electric Field,” in *Spin Wave Confinement: Propagating Waves (2nd Edition)*, edited by S. O. Demokritov (Pan Stanford Publishing Pte. Ltd., 2017) pp. 385–426.
- [23] G. A. Melkov, A. A. Serga, V. S. Tiberkevich, Yu. V. Kobljanskij, and A. N. Slavin, “Nonadiabatic interaction of a propagating wave packet with localized parametric pumping,” *Phys. Rev. E* **63**, 066607 (2001).
- [24] A. A. Serga, S. O. Demokritov, B. Hillebrands, Seong-Gi Min, and A. N. Slavin, “Phase control of nonadiabatic parametric amplification of spin wave packets,” *J. Appl. Phys.* **93**, 8585 (2003).
- [25] T. Brächer, F. Heussner, P. Pirro, T. Meyer, T. Fischer, M. Geilen, B. Heinz, B. Lägél, A. A. Serga, and B. Hillebrands, “Phase-to-intensity conversion of magnonic spin currents and application to the design of a majority gate,” *Sci. Rep.* **6**, 38235 (2016).
- [26] M. Weisheit, S. Fähler, A. Marty, Y. Souche, C. Poinsignon, and D. Givord, “Electric field-induced modification of magnetism in thin-film ferromagnets,” *Science* **315**, 349 (2007).
- [27] C.-G. Duan, J. P. Velev, R. F. Sabirianov, Z. Zhu, J. Chu, S. S. Jaswal, and E. Y. Tsymlal, “Surface magnetoelectric effect in ferromagnetic metal films,” *Phys. Rev. Lett.* **101**, 137201 (2008).
- [28] J. Zhu, J. A. Katine, G. E. Rowlands, Y.-J. Chen, Z. Duan, J. G. Alzate, P. Upadhyaya, J. Langer, P. K. Amiri, K. L. Wang, and I. N. Krivorotov, “Voltage-Induced Ferromagnetic Resonance in Magnetic Tunnel

- Junctions,” *Phys. Rev. Lett.* **108**, 197203 (2012).
- [29] Y.-J. Chen, H. K. Lee, R. Verba, J. A. Katine, I. Barsukov, V. Tiberkevich, J. Q. Xiao, A. N. Slavin, and I. N. Krivorotov, “Parametric Resonance of Magnetization Excited by Electric Field,” *Nano Letters* **17**, 572–577 (2017).
- [30] R. Verba, M. Carpentieri, G. Finocchio, V. Tiberkevich, and A. Slavin, “Excitation of Spin Waves in an In-Plane-Magnetized Ferromagnetic Nanowire Using Voltage-Controlled Magnetic Anisotropy,” *Phys. Rev. Applied* **7**, 064023 (2017).
- [31] R. Verba, M. Carpentieri, G. Finocchio, V. Tiberkevich, and A. Slavin, “Amplification and stabilization of large-amplitude propagating spin waves by parametric pumping,” *Appl. Phys. Lett.* **112**, 042402 (2018).
- [32] N. Bloembergen, *Nonlinear optics* (Addison-Wesley Pub. Co., 1965).
- [33] R. Verba, V. Tiberkevich, and A. Slavin, “Influence of interfacial Dzyaloshinskii-Moriya interaction on the parametric amplification of spin waves,” *Appl. Phys. Lett.* **107**, 112402 (2015).
- [34] L. Lopez-Diaz, D. Aurelio, L. Torres, E. Martinez, M. A. Hernandez-Lopez, J. Gomez, O. Alejos, M. Carpentieri, G. Finocchio, and G. Consolo, “Micromagnetic simulations using Graphics Processing Units,” *J. Phys. D: Appl. Phys.* **45**, 323001 (2012).
- [35] V. Puliafito, A. Giordano, A. Laudani, F. Garesci, M. Carpentieri, B. Azzerboni, and G. Finocchio, “Scalable synchronization of spin-Hall oscillators in out-of-plane field,” *Appl. Phys. Lett.* **109**, 202402 (2016).
- [36] T. Maruyama, Y. Shiota, T. Nozaki, K. Ohta, N. Toda, M. Mizuguchi, A. A. Tulapurkar, T. Shinjo, M. Shiraishi, S. Mizukami, Y. Ando, and Y. Suzuki, “Large voltage-induced magnetic anisotropy change in a few atomic layers of iron,” *Nature Nano.* **4**, 158 (2009).